



Effects of Chemical Dispersants on Oil Physical Properties and Dispersion

Ali Khelifa, Merv Fingas, Bruce P. Hollebone, and Carl E. Brown
Emergencies Science and Technology Division
Environmental Science and Technology Centre, Science and Technology Branch
Environment Canada, Ottawa, ON, Canada
ali.khelifa@ec.gc.ca

Abstract

New laboratory experiments were performed to measure the effects of chemical dispersants on oil physical properties and dispersion. Specifically, the aims of this study were to measure the effects of dispersant-to-oil ratio (DOR) on the viscosity of crude oils, the brine-oil interfacial tension (IFT) and the related size distributions of oil droplets formed under various mixing conditions. Arabian Medium, Alaska North Slope and South Louisiana crude oils and Corexit 9500 and Corexit 9527 chemical dispersants were used to perform the study. Results showed a monotonous linear increase of oil viscosity with DOR. The increase is higher with the less viscous oils than with the more viscous oils. With increases in DOR from 0 to 1:5, oil-dispersant mixture viscosity is approximately 20, 30 and 40 % greater than the pure crude oils for Arabian Medium, Alaska North Slope, and South Louisiana crude oils, respectively. Similar results were obtained with both chemical dispersants. As reported in previous studies, application of chemical dispersants reduces the interfacial tension significantly for all values of DOR examined in the current study including a very low value of 1:200. For instance, the interfacial tension of Arabian Medium crude decreases from 20 mN/m to less than 3.6 mN/m (the detection limit of the instrument) at DOR=1:200. The results also show that an optimum DOR exists at which the IFT reduction reaches a maximum value. At this optimum DOR, the effectiveness of the chemical dispersant is at a maximum. The consequent effects of the observed IFT reductions on the resulting size distribution of oil droplets was studied using existing theories and size measurements using UV Epi-fluorescence microscopy.

1 Introduction

It is general knowledge that chemical dispersants affect oil dispersion via modification of the interfacial properties of the oil, such as oil-brine interfacial tension (IFT) (NAS, 2005). The end results of these modifications are a reduction of the size and enhancement of the concentration of oil droplets in the water column. This is well known from both laboratory and field testing. This is also illustrated by the existing theories related to the mechanics of formation of oil droplets (Hinze, 1975; Khelifa et al., 2004; Li and Garrett, 1998) and interfacial thermodynamics (NAS 2005, Liu et al., 1995). According to these theories, the reduction of IFT combined with the provision of sufficient mixing energy is one of the key ways to explain observed the reduction of droplet size of chemically treated oil (NAS, 2005). Several laboratory investigations on IFT reduction due to the application of chemical dispersants have been performed during the last few decades (Rewick et al. 1980, 1981, 1983, 1984; Mackay and Hussein, 1982; Clayton, 1993; Liu et al., 1995). All these studies showed a reduction of IFT with the addition of chemical dispersants. Factors such as oil type, dispersant type and dispersant to oil ratio (DOR) were identified as important factors affecting the magnitude of IFT reduction. However,

extrapolation of this information to practical application, such as modelling of oil droplet formation is still not well developed due, apparently, to a poor understanding of the process and the lack of representative data sets. The aim of this paper is to present new laboratory results on the effects of chemical dispersants on IFT and oil viscosity and the subsequent effects on oil droplet formation.

2 Effects on physical properties of oil

The experiments were conducted using three oils: Arabian Medium (AM), Alaska North Slope (ANS) and South Louisiana (SL) crude and Corexit 9500 and Corexit 9527 chemical dispersants. All the experiments were performed at a controlled temperature of 15 °C. The density of the oils and dispersants were measured using an Anton Parr DMA 5000 digital densitometer. The instrument was factory-calibrated. Results are shown in Table 1. Note that the dispersants are denser than any of the three oils considered in this study. Uncertainty in measurements is estimated from the standard deviation of at least eight trials of *p*-xylene at 15.0 °C. Estimated uncertainty in density measurements is ± 0.002 at a 95% confidence level.

Table 1. Measured Oil Densities

Oil/Dispersant	Density (g/mL)
Alaska North Slope	0.873
Arabian Medium	0.876
South Louisiana	0.859
Corexit 9500	0.959
Corexit 9527	1.002

Oil dynamic viscosity was measured with a Thermo-Haake VT550 viscometer using NV cup-and-spindle sensors. The instrument was factory-calibrated and the calibration verified with ASTM-traceable standards (Cannon Instrument Co.) at 15.0 °C. Pure ethylene glycol (Caledon Laboratory Ltd.) is used to validate the NV method. Estimated uncertainty with this instrument is ± 1.3 mPa s at a 95% confidence level. For each of the three oils, viscosity measurements are repeated in triplicate for dispersant-to-oil ratios (DOR) of 0, 1:40, 1:20, 1:10, 1:5, and dispersant only. Results are listed in Table 2. All oils show an increase of oil viscosity with DOR. As summarized in Table 2 and shown in Figure 1, results show that when DOR increases from 0 to 1:5, the viscosity of the oil-dispersant mixture increased with an increasing amount of dispersant. The relative increases ranged from about 15% with Arabian Medium and Corexit 9500 to about 43 % with South Louisiana crude and Corexit 9527 over the crude oil viscosities. The linear trend in viscosity increases with increasing DOR suggest that the viscosity of the mixture is related to a linear proportion of the less viscous crude oils and the more viscous dispersants. Both dispersants showed similar increases in oil viscosity with DOR.

Surface and oil-water interfacial tensions were measured using a Krüss K10 Tensiometer by the Du Noüy ring method. Measurements were made at 15.0 °C, maintained by an external temperature-regulating bath (Thermo Haake). Samples, aqueous phases and glassware are all maintained at 15.0 °C for a minimum of 30 minutes before measurement. The instrument was factory calibrated and instrument calibration was verified using a vendor-supplied weight. Method and operator

performance is monitored by periodic measurement of the surface and liquid/liquid interfacial tensions of *p*-xylene at 15.0 °C.

For oil/air surface tensions, the measurement ring is first zeroed in air. A small amount of sample, approximately 15 mL, is poured into a 43-mm diameter vessel (50 mL Kimax beaker). The ring is dipped into the sample to a depth of no more than 5 mm, and then pulled up such that it is just visible on the surface of the liquid. Measurement is automatically terminated when the upward pulling force on the ring just balances the downward force exerted by the liquid meniscus. The apparent interfacial tension, σ_{o-a}^{APP} , is then recorded.

Table 2. Measured Viscosities of different Oil and Dispersant Mixtures

Oil/Dispersant Mixture	Viscosity (mPa s) for DOR by weight:					
Fresh Oil	0	1:40	1:20	1:10	1:5	dispersant only
Alaska North Slope	17.0					
Arabian Medium	28.1					
South Louisiana	13.3					
Fresh Oil + Corexit 9500						
Alaska North Slope	17.8	18.0	20.0	23.7		
Arabian Medium	29.4	28.1	29.8	32.4		
South Louisiana	13.7	14.7	16.0	18.2		
Fresh Oil + Corexit 9527						
Alaska North Slope	17.7	17.8	20.3	22.5		
Arabian Medium	28.1	28.4	29.5	33.5		
South Louisiana	13.8	14.4	15.1	19.0		
Corexit 9500						92.9
Corexit 9527						67.5

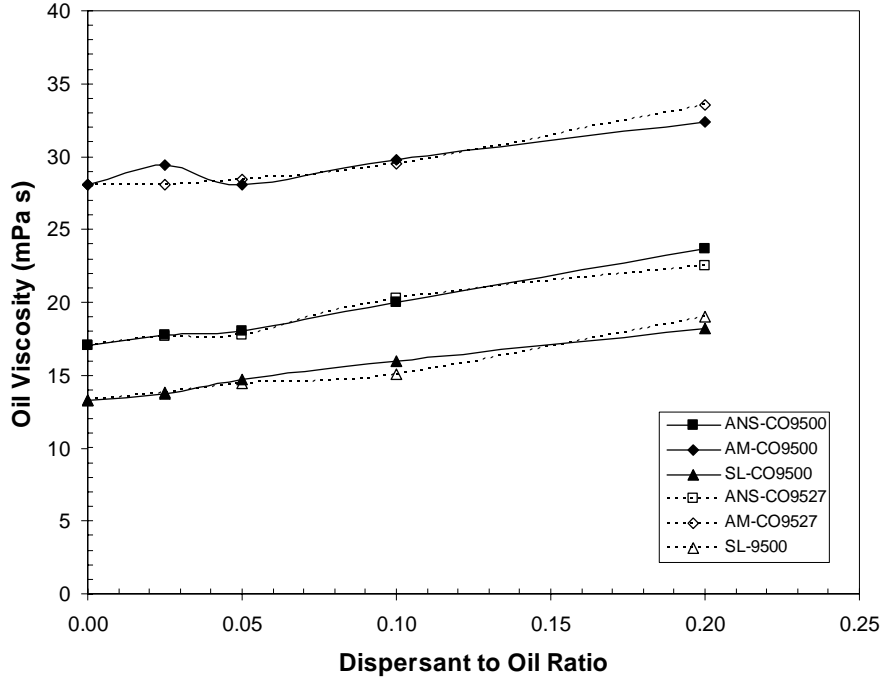


Figure 1. Measured variations of oil viscosity with dispersant to oil ratio.

For brine/oil interfacial tensions, the ring is zeroed in the sample oil at a depth of 5 mm. The ring is removed and cleaned. A 25-mL volume of water or brine is dispensed into a 43-mm diameter vessel. The ring is dipped 5 mm into the aqueous phase. A 10-mL volume of sample is carefully poured down the side of the vessel wall (creating a 10-mm thick layer of sample on the water), with great care taken so as to disturb the aqueous/oil interface as little as possible. The ring is then raised to the bottom on the interface and the system is allowed to rest for exactly 30 seconds. The measurement is started and the apparent interfacial tension is recorded, σ_{o-w}^{APP} , when the force balance is reached.

The apparent surface tension is corrected for the mass of the upper phase lifted by the ring during measurement using the Zuidema and Waters correction:

$$\sigma_{o-w} = \sigma_{o-w}^{APP} \left(0.7250 + \sqrt{\frac{1.452\sigma_{o-w}^{APP}}{D_{DN}^2(\rho_{inf} - \rho_{sup})} - \frac{1.679}{D_{DN}/D_{rw}} + 0.04534} \right) \quad (1)$$

where: σ_{o-w} is the oil-water interfacial tension, σ_{o-w}^{APP} is the instrument scale reading, ρ_{inf} is the density of the lower phase, ρ_{sup} is the density of the upper phase, D_{DN} is the diameter of the Du Noüy ring, and D_{rw} is the diameter of the ring wire.

Measurements are repeated in triplicate, or more, if required. The mean of at least three corrected interfacial tensions is reported as the measured value. Measured surface (oil/air) and interfacial (brine/oil) tensions for 33‰ brine are shown in Table 3 for the fresh oils. For the surface tensions (oil/air), estimated uncertainty is ± 1.2 mN/m at a 95% confidence level. The limit of detection (3 times the standard deviation) is 1.8 mN/m. For the brine/oil interfacial tensions, estimated uncertainty is ± 2.5 mN/m at a 95% confidence level. The limit of detection is 3.6 mN/m.

Table 3. Measured Surface (oil/air) and Interfacial (brine/oil) Tensions without Chemical Dispersants

Fresh Oil	Surface Tension (mN/m)	Brine/Oil Interfacial Tension (mN/m)
Alaska North Slope	26.4	19.0
Arabian Medium	26.5	20.0
South Louisiana	26.5	16.2

Brine/oil interfacial tensions for oils mixed with dispersants were below the detection limit, i.e. <3.6 mN/m, for all DOR values and for both dispersants (Corexit 9500 and Corexit 9527). Additional diluted mixtures with DOR of 1:200 were prepared for both dispersants and for all three oils to test further the observed effects of dispersants. No measurements of brine/oil interfacial tension could be determined even for these more dilute mixtures. As shown in Figure 2, a simple mixing test was performed with fresh South Louisiana oil and Corexit 9500 at DOR of 1:200 to quickly test these results on oil dispersion. Fresh oil and oil-dispersant mixtures were layered on the top of 33% brine solution in small beakers (Figure 2a) and then mixed vigorously (manually) for about one minute. As shown in Figure 2b, even at a DOR of 1:200 oil-dispersant mixture dispersed much easier than the fresh oil. Such increase in oil dispersion, i.e. transformation of the oil layer into small droplets in the water column, relates to a reduction of the oil-water interfacial tension. Mackay and Hussein (1992) estimated (assuming exponential decay of IFT with DOR) that a 1:500 DOR of Corexit 9527 is sufficient to reduce the IFT of various crude oil to 20-fold. Liu et al. (1995) measured about a 1000-fold reduction in IFT when the DOR increases from 1:200 to 1:10. All of these results are in qualitative agreement with measurements found in the present study.

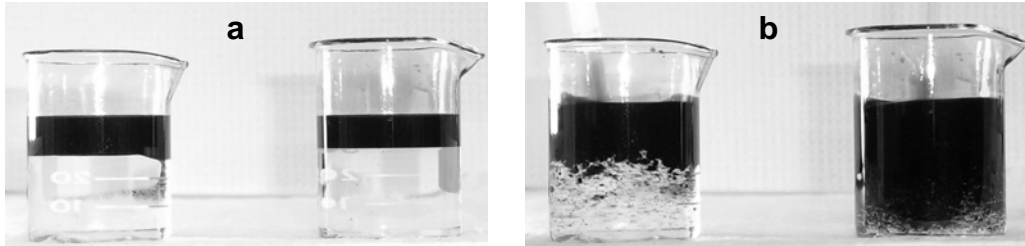


Figure 2. Simple dispersion testing: South Louisiana before (a) and after (b) 1 minute mixing. In each of these pictures, the left beaker contains no dispersant and the right one has Corexit 9500 at 1:200 DOR

3 Effects on oil dispersion

The effects of a reduction in the IFT on droplet formation can easily be illustrated using existing theories. From a thermodynamic point of view, the change in the free energy of the system after dispersion of an oil slick of thickness η to oil droplets for diameter D can be expressed by (Liu et al. 1995):

$$\Delta E = \sigma_w + \sigma_{o-w} \left(6 \frac{\eta}{D} - 1 \right) - \sigma_o \quad (2)$$

where σ_w and σ_o represent surface tension of water and oil, respectively.

As such, dispersion of an oil slick into the water column requires reduction of ΔE as described in equation (2). ΔE is proportional to IFT reduction and the thickness of the slick and is inversely proportional to the size of the dispersed droplets. From the droplet formation perspective, existing theories show that IFT is a key factor that controls the size of oil droplets. This may be shown considering the model discussed by Khelifa et al. (2005) and described by equation (3). Computed reductions of maximum droplet size with the reduction of IFT are shown in Figure 3 for moderate ($1 \text{ m}^2/\text{s}^3$) and high ($10 \text{ m}^2/\text{s}^3$) kinetic energy dissipation rates ε .

$$D_{\max} = \begin{cases} 0.726 \left(\frac{\sigma_{o-w}}{\rho_w} \right)^{3/5} \varepsilon^{-2/5} & \text{for } \varepsilon \leq \varepsilon_c \\ 5.2 \times 10^{-5} \left(\frac{\sigma_{o-w}}{\rho_w \nu_w} \right)^3 \varepsilon^{-1} \left(\frac{\rho_o \nu_o}{\rho_w \nu_w} \right)^{3/8} & \text{for } \varepsilon > \varepsilon_c \text{ and } D_{\max} \geq \kappa \\ 3.8 \times 10^{-2} \left(\frac{\sigma_{o-w}}{\rho_w \nu_w} \right) \nu^{0.5} \varepsilon^{-1/2} \left(\frac{\rho_o \nu_o}{\rho_w \nu_w} \right)^{1/8} & \text{for } \varepsilon > \varepsilon_c \text{ and } D_{\max} < \kappa \end{cases} \quad (3)$$

where D_{\max} is the maximum droplet size, σ_{o-w} oil-water interfacial tension, ρ_w water density, ρ_o oil density, ε kinetic energy dissipation rate, ν_w kinematic viscosity of water, ν_o kinematic viscosity of oil, κ Kolmogorov length scale and $\varepsilon_c = (7.2 \times 10^{-5})^{5/3} (\sigma_{o-w} / \rho_w \nu_w)^5 (\sigma_{o-w} / \rho_w)^{-1} (\rho_o \nu_o / \rho_w \nu_w)^{5/8}$. The first expression in equation (3) is the Hinze model which is assumed to describe droplet breakup at relatively low dissipation rates. The two other expressions represent the model proposed by Li and Garrett (1998) when the dissipation rate exceeds a value defined by ε_c . Similar model was used recently by Tkalic and Chan (2002) to investigate vertical mixing of oil droplets under breaking wave conditions

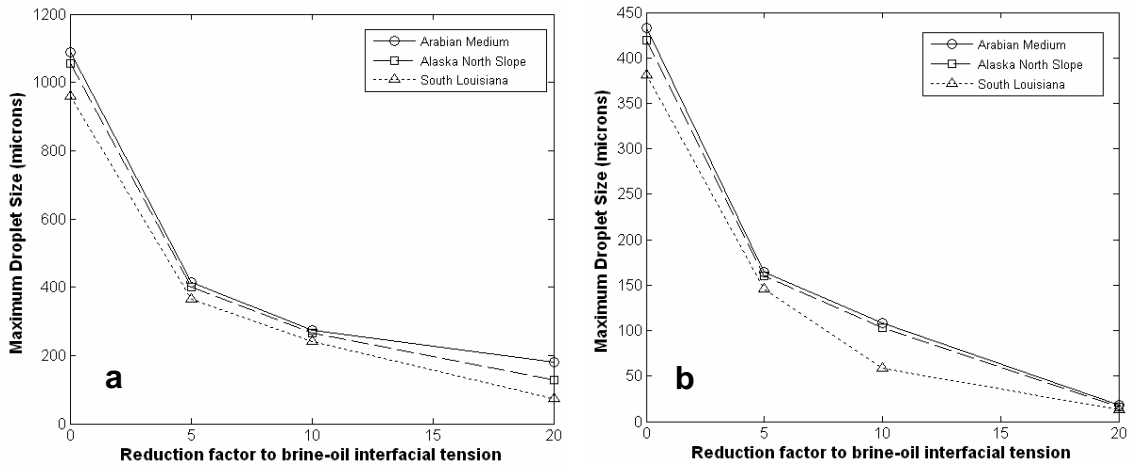


Figure 3: Calculated decrease of maximum oil droplet size with the reduction of brine-oil interfacial tension for kinetic energy dissipation rate $\varepsilon = 1 \text{ m}^2/\text{s}^3$ (a) and $10 \text{ m}^2/\text{s}^3$ (b) according to equation (3).

Further experiments were performed to measure the effects of IFT reduction on oil droplet size distribution. About 50 mg of Alaska North Slope were mixed with 250 mL of brine (33%) in a reciprocating shaker for at least 90 minutes. Corexit 9500

was used at DOR of 0, 1:200, 1:100, 1:40, 1:20, and 1:10. While shaking, water samples were collected from the center of the suspension after about 90 minutes shaking. Each sample was analyzed immediately using UV-epi fluorescence microscopy equipped with a high resolution digital camera. The imaging setup is designed to detect oil droplets up to 0.1 μm in size.

Examples of microphotographs obtained from the imaging setup are shown in Figure 4. These microphotographs showed some interesting results about oil dispersion. The first one is that for DOR less than 1:100, the chemical dispersant has less effect on oil droplet size (Compare Figures 4e & f to 4a). The second one relates to the fact that the smallest oil droplets (generally used as an indicator of dispersant effectiveness) are not obtained at the highest DOR of 1:10 (Figure 4b), but at a DOR equal to 1:20 (Figure 4c). The third observation is that there is a good similarity between oil droplet populations obtained with DOR of 1:10 (Figure 4b) and 1:40 (Figure 4d). These observations were corroborated by visual evaluation of water turbidity (Figure 5) and quantitatively by measurements of droplet size distributions. The later was performed using an in-house image analysis program developed on the Matlab platform. A minimum of 15 frames were evaluated in the analysis depending on the concentration of oil droplets. Visual diagnosis of the six samples shown in Figure 5 clearly confirm that the 1:20 DOR provided the highest oil dispersion (highest turbidity). Water samples for DOR equal to 1:100 and less are clear and comparable to water sample without dispersant. This is further confirmation of what was observed in Figure 4. Large oil droplets resurface faster than small droplets, which makes the water samples at low DOR look cleaner than at higher DOR.

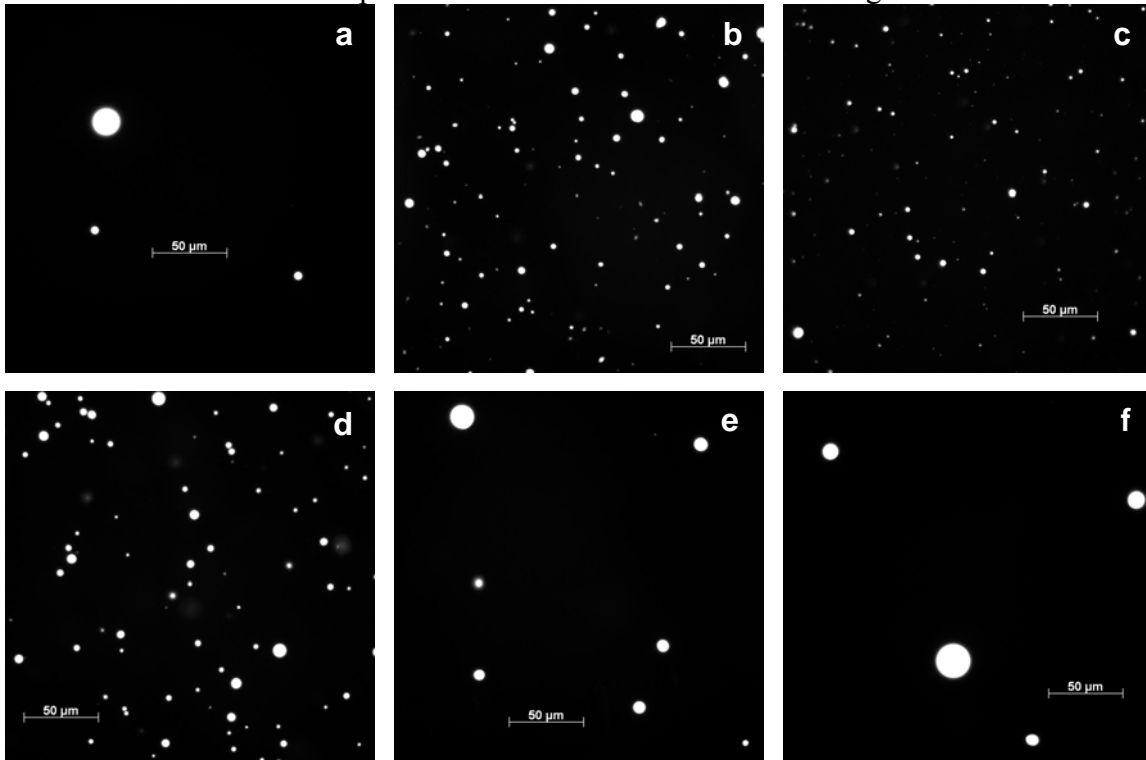


Figure 4: Microphotographs of oil droplets measured after 90 minutes while shaking using UV epi-fluorescence microscopy, Alaska North Slope crude and Corexit 9500 at various DOR: no dispersant (a), 1:10 (b), 1:20 (c), 1:40 (d), 1:100 (e), 1:200 (f).

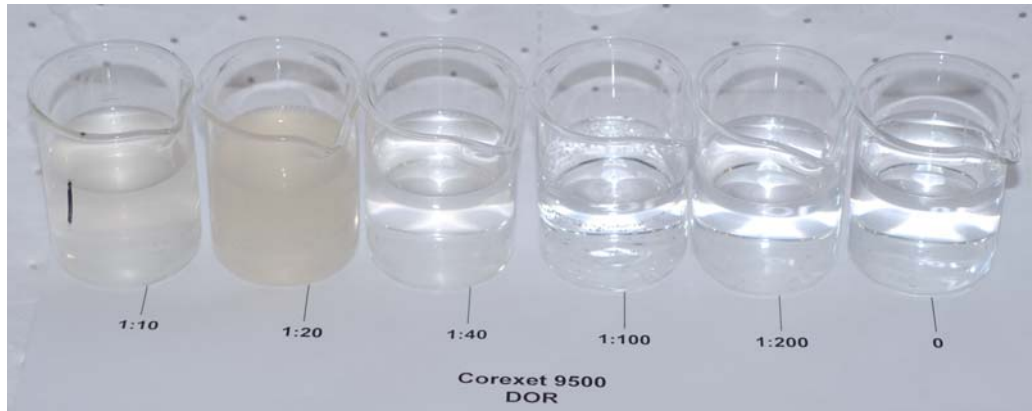


Figure 5: Water samples from different reaction chambers after overnight settling period. The ratios shown in this figure represent DOR values. Alaska North Slope crude and a shaking period of about 90 minutes. Clear water samples showed that most of the dispersed oil in the water column has resurfaced in the reaction chamber during the settling period.

One way to quantitatively investigate the observations discussed above is to measure droplet size distributions during shaking and after different settling periods. This is shown in Figure 6. All measured size distributions are shown in number concentration. Results shown in Figure 6a confirm observations made above from Figure 4. The highest concentration of small oil droplets are shown with DOR 1:20 during shaking and after the two settling periods. Size distributions measured with DOR 1:10 and 1:40 are very similar. For small DOR, size distributions measured while shaking are comparable to no dispersant conditions and include the largest droplets of about $25\mu\text{m}$ (Figure 6a). Comparison between droplet concentration in Figures 6a and 6b showed that coalescence between chemically dispersed oil droplets does occur, as more large droplets and less small droplets were measured at high values of DOR. After overnight settling period, during which large droplets have reached the water surface (Fingas and Decola, 2006), almost all size distributions are within the same size range between 0.3 and $7\mu\text{m}$. The high concentration of small droplets shown in Figure 6c for DOR=1:20 (higher than during shaking, Figure 6a) was not expected and is probably due to a contamination of the syringe during the sampling process.

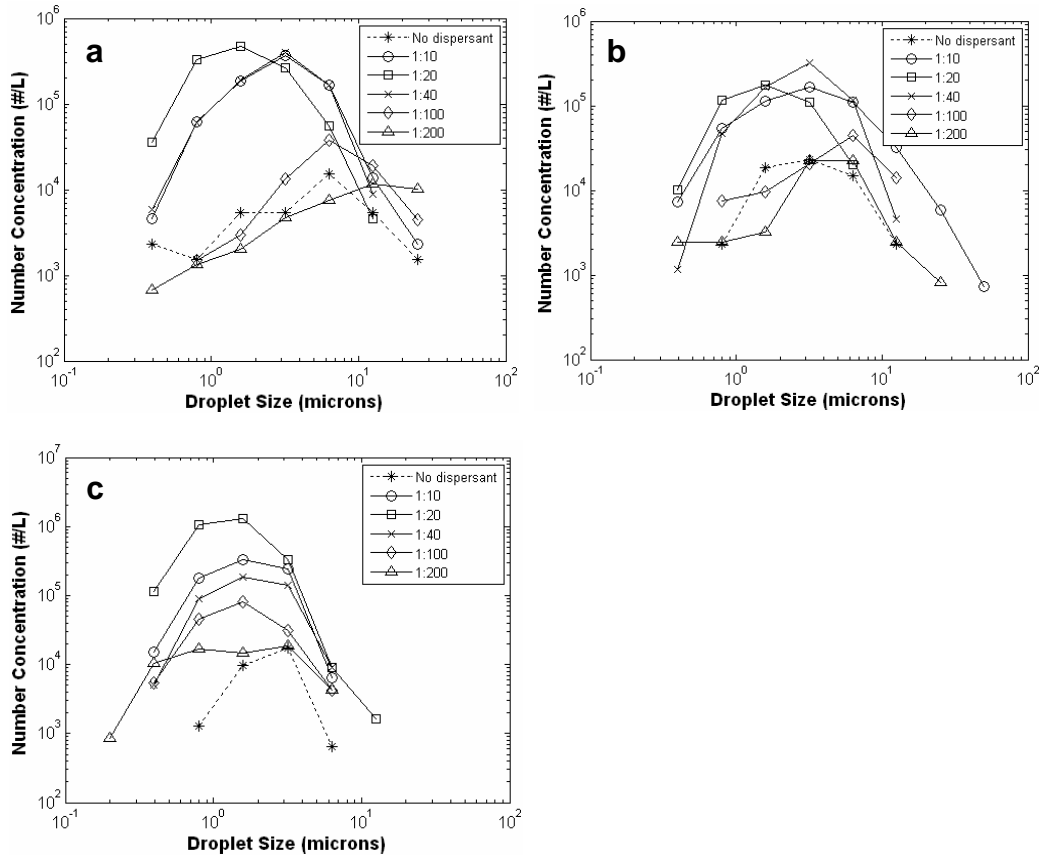


Figure 6: Measured droplet size distributions using UV epi-fluorescence microscopy, Alaska North Slope crude and Corexit 9500 at various DOR after 90 minutes shaking (a), 90 minutes settling (b), and overnight settling (c).

Overall, the measured droplet size distributions confirm the visual observations discussed above. Further confirmation is also provided in the measured variations of median droplet size with DOR (Figure 7). The smallest median diameter of less than $2 \mu\text{m}$ was obtained with DOR=1:20. At the highest DOR of 1:10, measured median droplet size is about $3.2 \mu\text{m}$ during shaking and after 90 minutes settling period. Median size is almost constant at about $1.9 \mu\text{m}$ after overnight settling regardless of DOR, except for physically dispersed oil. A significant increase (about double) of the median size was observed when the DOR increased from 0 to 1:200 (during shaking) and 1:100 after 90 minutes settling was not expected. The authors have no explanation for these results at the current time.

It is interesting to note that the results obtained in this study are also in agreement with laboratory measurements discussed by Liu et al. (1995). Both visual and quantitative investigations showed in the present study show that Corexit 9500 is more effective in dispersing Alaska North Slope crude at DOR 1:20 (or 5%) than at a higher DOR of 1:10. For the two different types of chemical dispersants employed (noted No. 2 and No. 4 in their manuscript), Liu et al. (1995) measured a maximum reduction of IFT at a DOR of 6% (or 1:17), while for the two other chemical dispersants they studied (No. 1 and No. 2), they measured a monotonous decrease of IFT with DOR. The DOR value at which the IFT reached a maximum reduction (1:20 in the present study and about 1:17 in Liu et al, 1995) is considered as the

approximate critical micelle concentration (CMC) of chemical dispersant. Apparently, this concentration is a function of the type and solubility of chemical dispersant, oil type, and oil to water ratio, but very little is known about this concentration. More laboratory measurements are needed to fully understand the effect of this parameter on dispersant effectiveness.

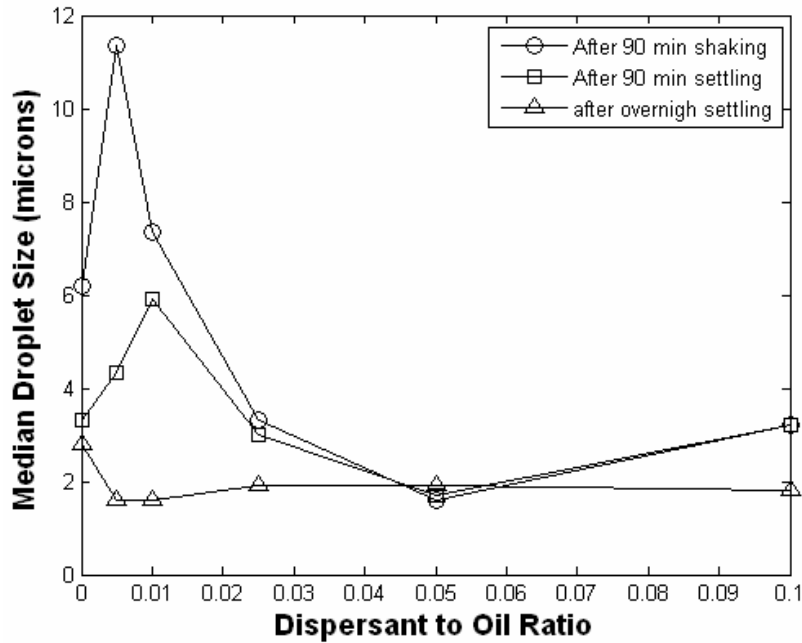


Figure 7. Median Droplet Size versus Dispersant to Oil Ratio (DOR)

4 Conclusion

Several interesting observations were made in this study. It was shown that brine-oil interfacial tension associated with Arabian Medium, Alaska North Slope and South Louisiana crudes reduces to less than 3.6 mN/m with the application of chemical dispersants Corexit 9500 and 9527, even at a low DOR value of 1:200. The Du Noüy ring method is not an appropriate method to measure small IFT values. The application of chemical dispersants increases the viscosity of the dispersant-oil mixture up to 40% over the neat crude oil. Using a high resolution imaging setup, the effect of IFT reduction on oil dispersion was measured and showed significant reduction of size and enhancement of the concentration of oil droplets, as predicted by existing theories. However, this study showed that for each mixing condition, an optimum value of DOR exists that provides for maximal dispersant effectiveness. At this optimum DOR, the IFT appeared to reach a maximum reduction, as inferred from the droplet size. This finding is in agreement with results presented in a previous study and suggests that the optimum DOR corresponds to the critical micelle concentration (CMC) of the chemical dispersant. For an Alaska North Slope/Corexit 9500 combination, the optimum DOR is 1:20. Above and below this concentration, the size of the oil droplets increases and their concentration decreases in the water column. Further investigation of IFT reduction with DOR and variations of CMC with the type and the solubility of chemical dispersant, oil type, and oil to water ratio would certainly benefit the oil spill community from a number of different perspectives. For instance, very little is known on how to integrate the effects of

chemical dispersants into oil spill models. Better quantification of this quantity is critical to a better understanding of oil-dispersant interaction. The benefit of this procedure to the actual method that looks to the reduction of droplet size distribution is that, the size reduction of chemically dispersed oil droplets is a result of a (non linear) combination of at least the chemical effects of the chemical dispersant and the physical effects dictated by the turbulent mixing.

5 Acknowledgements

Funding for this project was provided by the Coastal Response Research Center www.crrc.unh.edu

6 References

- Clayton, J.R., J.R. Payne, and J.S. Farlow, "Oil Spill Dispersants: Mechanisms of Action and Laboratory Tests", *CRC Press*, Boca Raton, 1993, p. 103.
- Fingas, M. and E. Decola, "Oil Spill Dispersant Effectiveness Testing in OHMSETT", Report submitted to Prince William Sound Regional Citizens' Advisory Council (PWSRCAC), Anchorage, Alaska, 47p., 2006.
- Hinze, J.O., "Fundamentals of the hydrodynamic mechanism of splitting in dispersion processes", *AIChE Journal*, Vol. 8 (4), 289-295, 1955.
- Khelifa, A., P.S. Hill, and K. Lee, "A Comprehensive Numerical Approach To Predict Oil-Mineral Aggregate (OMA) Formation Following Oil Spills In Aquatic Environments", in: *Proceedings of the 2005 International Oil Spill Conference*, American Petroleum Institute, Miami Beach, Florida, 2005.
- Khelifa, A., P.S. Hill, and K. Lee, "Prediction of Oil Droplet Size Distribution in Agitated Aquatic Environments", in *Proceedings of the 27th Arctic and Marine OilSpill Program (AMOP) Technical Seminar*, Environment Canada, Ottawa, ON, Canada, pp. 371-382, 2004.
- Li, M., and C. Garrett, "The Relationship Between Oil Droplet Size and Upper Ocean Turbulence", *Marine Pollution Bulletin*, 36(12), pp. 961-970, 1998.
- Liu, H., Y. Zhang, and W. Wang, "Interfacial Properties Of Oil Spill Dispersants And Their Effects On Dispersion Effectiveness", *Acta Oceanologica Sinica*, pp. 587-593, 1995
- Mackay, D. and K. Houssain, "Oil-Water Interfacial Tensions In Chemical Dispersant", *Report EE-32*, Environment Canada, Ottawa, 17p, 1982.
- NAS, *Oil Spill Dispersants: Efficacy and Effects*, National Academy of Sciences, Washington, D.C., 330 p and Annexes, 2005.
- Rewick, R. T., K. A. Sabo and J. H. Smith, "The Drop-weight Interfacial Tension Method for Predicting Dispersant Performance", *Oil Spill Chemical Dispersants, Research Experience and Recommendations, ASTM STP 840*, American Society for Testing Materials, Philadelphia, PA, pp. 94-107, 1984.
- Rewick, R.T., K.A. Sabo, J. Gates, J.H. Smith and L.T. McCarthy, "An Evaluation Of Oil Spill Dispersant Testing Requirements", in *Proceedings of the 1981*

International Oil Spill Conference, Atlanta, Georgia, American Petroleum Institute, pp. 5-10, 1981.

Rewick, R.T., G. Jennifer, and H.S. James, "Simple Test Of Dispersant Effectiveness Based On Interfacial Tension Measurements, *Fuel*, Vol. 9, pp. 263-265, 1980.

Tkalich, P., and E.S. Chan, "Vertical Mixing of Oil Droplets by Breaking Waves", *Marine Pollution Bulletin*, 44 (11), pp. 1219-1229, 2002.